N^1-Alkylated Pyrimidine Films as a New Potential Optical Data Storage Medium

Brian Lohse,[†] Søren Hvilsted,[‡] Rolf H. Berg,*[,†] and P. S. Ramanujam*[,§]

Polymer Department and Optics and Plasma Research Department, Risø National Laboratory, DK-4000 Roskilde, Denmark, and the Danish Polymer Centre, Department of Chemical Engineering, Technical University of Denmark, DK-2800 Kgs. Lyngby, Denmark

Received May 10, 2006. Revised Manuscript Received August 4, 2006

We investigate several compounds of the type 1,1′-(α,ω-alkanediyl)bis[pyrimidine] and 1-(ω-bromoalkyl)uracil, which can undergo photoinduced ($2\pi + 2\pi$) cycloaddition reactions on exposure to UV light at 254 and 257 nm, which have been synthesized for application in high capacity optical data storage. Their dimerization efficiency was compared, in solution, with uracil as a reference, and as films, to investigate the correlation between solution and film. Films of good quality displaying excellent thermal and optical stability can be fabricated. A significant optical contrast between the irradiated and nonirradiated medium was observed. 1,1′-(1,3-Propanediyl)bis[uracil], 1,1′-(1,8-octanediyl)bis[uracil], and 1-(6-bromohexyl)uracil showed remarkably good dimerization efficiency and are a significant improvement compared to previously reported similar systems. Gray scale and holographic grating storage are also demonstrated in the films. Writing and reading of the gray scale can be performed at the same wavelength.

Introduction

Ultrahigh capacity archival storage is an important 21st century requirement for the information technology industry. Currently, a storage capacity of approximately 25 GB at 405 nm has been achieved on a 5.25 in. disk in the Blu-Ray system. One way of increasing the storage capacity is to employ even shorter wavelengths. This demands a new type of system to be implemented, based on a new technology to store data. Furthermore, for optimal storage, writing and reading should be performed at the same wavelength.

A significant effort has been put into finding a new type of optical data storage media, consisting of synthetically simple organic materials and thereby achieving higher data storage capacity.[1] Previous work has been done by synthesizing di- and oligopeptides,[2] where storage was achieved through photoinduced ($2\pi + 2\pi$) cycloaddition reactions on exposure to UV light at 254 and 257 nm. The compounds with good dimerization efficiency were made as thin films and tested, using a UV laser, showing interesting properties.[3] Recording of gray levels has been shown to be possible in thin films leading to the theoretical possibility of a storage capacity of 1 terabyte.[4] Two major problems with this technology have been unsolved for quite some time: (a) the quality of the film, which is extremely important when working with optical data storage, and (b) the writing speed in the media. This work is based on the same photochemical principles mentioned,[2−4] using N^1-alkylated pyrimidines instead of peptides. Here 1,1′-(α,ω-alkanediyl)bis[uracil], 1,1′-(α,ω-alkanediyl)bis[5-bromouracil], 1-(ω-bromoalkyl)-uracil, and 1-undecyl uracil were prepared, and the effect of the dimerization efficiency when increasing the carbon numbers (3−12) in the polymethylene chains was studied. The photodimerization process is shown for the 1,1′-(α,ω-alkanediyl)bis[pyrimidine] and the 1-(ω-bromoalkyl)pyrimidine species, in Figures 1 and 2, respectively.

Results

Preparation of 1,1′-(α,ω-Alkanediyl)bis[uracil] and 1,1′-(α,ω-Alkanediyl)bis[5-bromouracil]. Previously 1,1′-(α,ω-alkanediyl)bis[pyrimidine] has been synthesized through the reaction of a pyrimidine with 1-(ω-bromoalkyl)pyrimidine[5,6] for the purpose of studying base−base interactions. The preparation of 1-(ω-bromoalkyl)pyrimidine through a treatment of 2,4-bis(trimethylsilyloxy)pyrimidines and α,ω-dibromoalkane[5,6−8] has been reported. Later a more direct

* To whom correspondence should be addressed. E-mail: rolf.berg@risoe.dk (R.H.B.); p.s.ramanujam@risoe.dk (P.S.R.)

[†] Polymer Department, Risø National Laboratory.

[‡] Technical University of Denmark.

[§] Optics and Plasma Research Department, Risø National Laboratory.

(1) (a) Berg, R. H.; Hvilsted, S.; Ramanujam, P. S. *Nature* **1996**, *383*, 505−508. (b) Rasmussen, P. H.; Ramanujam, P. S.; Hvilsted, S.; Berg, R. H. *J. Am. Chem. Soc.* **1999**, *121*, 4738−4743. (c) Gabor, D. *Nature* **1948**, *161*, 777−778. (d) Gabor, D. *Science* **1972**, *177*, 299−313. (e) Natansohn, A.; Rochon, P.; Gosselin, J.; Xie, S. *Macromolecules* **1992**, *25*, 2268−2273. (f) Meerholz, K.; Volodin, B. L.; Sandalphon; Kippelen, B.; Peyghambarian, N. *Nature* **1994**, *371*, 497−500.

(2) (a) Lohse, B.; Ramanujam, P. S.; Hvilsted, S.; Berg, R. H. *J. Pept. Sci.* **2005**, *11*, 499−505. (b) Lohse, B.; Ramanujam, P. S.; Hvilsted, S.; Berg, R. H. *J. Photochem. Photobiol., A* **2006**, submitted.

(3) Lohse, B.; Ramanujam, P. S.; Hvilsted, S.; Berg, R. H. *Jpn. J. Appl. Phys.* **2006**, *45* (1B), 488−492.

(4) Ramanujam, P. S.; Berg, R. H. *Appl. Phys. Lett.* **2004**, *85*, 1665−1667.

(5) Browne, D. T.; Eisinger, J.; Leonard, N. J. *J. Am. Chem. Soc.* **1968**, *90*, 7302−7323.

(6) Leonard, N. J.; McCredie, R. S.; Logue, M. W.; Cundall, R. L. *J. Am. Chem. Soc.* **1973**, *95*, 2320−2324.

(7) Tjoeng, F.-S.; Kraas, E.; Breitmier, E.; Jung, G. *Chem. Ber.* **1976**, *109*, 2615−2621.

(8) Nowick, J. S.; Chan, J. S.; Noronha, G. *J. Am. Chem. Soc.* **1993**, *115*, 7636−7644.

10.1021/cm061092f CCC: $33.50
Published on Web 09/06/2006

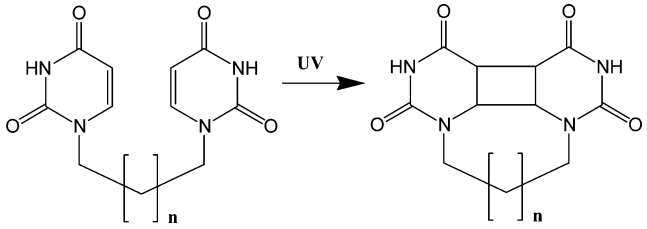

Figure 1. Photodimerization induced by UV light in 1,1′-(α,ω-alkanediyl)-bis[pyrimidine].

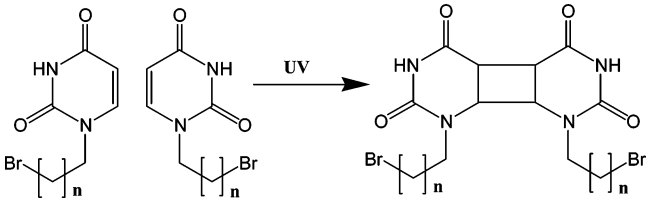

Figure 2. Photodimerization induced by UV light in 1-(ω-bromoalkyl)-pyrimidine.

method for the preparation of 1,1′-(α,ω-alkanediyl)bis[uracil] from uracil with α,ω-dibromoalkane had been described.[9] Here pyrimidines were treated with $Br(CH_2)_nBr$ ($n = 3-10$) in the presence of *t*-BuOK in dimethylformamide (DMF) resulting in the formation of 1,1′-(α,ω-alkanediyl)bis[pyrimidine] but also the 1-(ω-bromoalkyl)pyrimidine species, while similar treatment of pyrimidines in the presence of bases such as NaH, Cs_2CO_3, K_2CO_3, Na_2CO_3, and CH_3-COOK instead of *t*-BuOK did not give the 1,1′-(α,ω-alkanediyl)bis[pyrimidine];[10] we tried in addition to use KOH, Et_3N, and pyridine. KOH was found to give small amounts of mono N-alkylated pyrimidines. Furthermore, over 50% of the unalkylated pyrimidine was recovered in the reaction system.

Because we were also interested in the 1-(ω-bromoalkyl)-pyrimidine species, the existing methods only gave these as byproducts, meaning low yields, and the workup was time-consuming, we developed a direct method for N^1-alkylation of pyrimidines using the sterically hindered base 2,2,6,6-tetramethyl piperidine (TMP). The synthesis with TMP worked well giving the desired 1-(ω-bromoalkyl)pyrimidine species, in significantly higher yields (43−60%) than previously reported (23-30%[5] and 5−22%,[9] respectively). The 1-undecyl uracil was prepared in the same manner, or with K_2CO_3. The advantages are that TMP is easily dissolved in DMF, the reaction time was shorter, and it can be removed under vacuum.

It is well-known that the alkylation of pyrimidines can generally occur at the N^1 as well as the N^3 positions in the pyrimidine ring system,[11] although selective alkylation at the N^1 position is known.[12] Therefore, it is important to distinguish the difference between the structures of these two isomers at the N^1 and the N^3 positions. The structures of the two isomers was differentiated on the basis of the coupling constants between $H-C^5$ and $H-N^3$ of the N^1-substituted pyrimidines and between $H-C^6$ and $H-N^1$ of N^3-substituted pyrimidines and was found to be in accordance with results from the litterature.[9] We used two-dimensional NMR (2D-NMR) to verify the fact that it was a N^1 alkylation and not N^3. 2D-NMR experiments were done, and proton−proton cross-couplings were studied, clearly showing a nuclear Overhauser effect (NOE) between $H-C^6$ and $-CH_2-N^1$ of the N^1-alkylated pyrimidines synthesized, isolated, and used in these experiments. The 2D-NMR experiments were found to be unambiguous, and the NOE effect was found to be an excellent way of verifying that N^1 alkylations had taken place on the pyrimidines. The differentiation between N^1 and the N^3 alkylations based on coupling constants was found to be more time-consuming and often ambiguous. The reason for this ambiguity is that differentiation between isomers is greatly dependent on concentration, solvent, and temperature, which is also described in the literature.[9,13]

The chemical structures of the N^1-alkylated pyrimidine species prepared and investigated in this study are shown in Figure 3a−d. The 1,1′-(α,ω-alkanediyl)bis[uracil] species **1**−**6** are shown in Figure 3a, the 1,1′-(α,ω-alkanediyl)bis-[5-bromouracil] **7** and **8** are shown in Figure 3b, the 1-(ω-bromoalkyl)uracil **9**−**14** are shown in Figure 3c, and 1-undecyl uracil **15** is shown in Figure 3d.

All synthesized compounds **1**−**15** studied in solution had a concentration of approximately 600 μg in 1 mL of Milli-Q water and an absorbance of 1. Water proved to be the best solvent, although for the alkylated species ($n \geq 7$), heating was necessary. Furthermore, water's absorption does not interfere with the absorbance area of the pyrimidines. The dimerization experiments have been described in detail in a previous work.[2a]

The sample was measured before irradiation and after each irradiation period (15, 30, and 60 min), in a UV spectrophotometer giving an indication of the dimerization efficiency. The decrease in absorbance is an indication of how much of the compound in the solution has dimerized. The dimerization efficiency of the compounds **1**−**15** was investigated in this study. The significance of the methylene chain length was investigated by synthesizing pyrimidines with different N^1-alkylated chain lengths. The absorption spectra of pyrimidines show a strong peak at ∼260 nm, due to the 5,6-double bond. When two pyrimidines are converted to a dimer, the 5,6-bond is saturated and the absorption from the double bond decreases.

The absorbance of uracil, chosen as the reference, is shown in Figure 4a, before and after 15, 30, and 60 min of irradiation with UV light. The absorption for **1** is shown in Figure 4b, showing a significant increase in dimerization efficiency, as it was also observed in previous work when attaching uracil to peptides.[2]

5-Bromouracil was chosen, as it was found that the dimerization efficiency improved significantly when attached to peptides and no dehalogenation was observed with dipep-

(9) Itahara, T. *Bull. Chem. Soc. Jpn.* **1997**, *70*, 2239−2247.
(10) Itahara, T. *Bull. Chem. Soc. Jpn.* **1996**, *69*, 3239−3246.
(11) (a) Case, F. H.; Hill, A. J. *J. Am. Chem. Soc.* **1930**, *52*, 1536−1542. (b) Baker, B. R.; Chheda, G. B. *J. Pharm. Sci.* **1965**, 54, 25−30. (c) Martinez, A. P.; Lee, W. W. *J. Org. Chem.* **1965**, *30*, 317−318. (d) Itahara, T.; Fujii, Y.; Tada, M. *J. Org. Chem.* **1988**, *53*, 3421−3424.
(12) Yamauchi, K.; Kinoshita, M. *J. Chem. Soc., Perkin Trans. 1* **1973**, 391−392.
(13) (a) Philipsborn, V. W.; Altman, J.; Babad, E.; Bloomfield, J. J.; Ginsburg, D.; Rubin, M. B. *Helv. Chim. Acta* **1970**, 53, 725−731. (b) Poulter, C. D.; Anderson, R. B. *Tetrahedron Lett.* **1972**, 3823−3826.

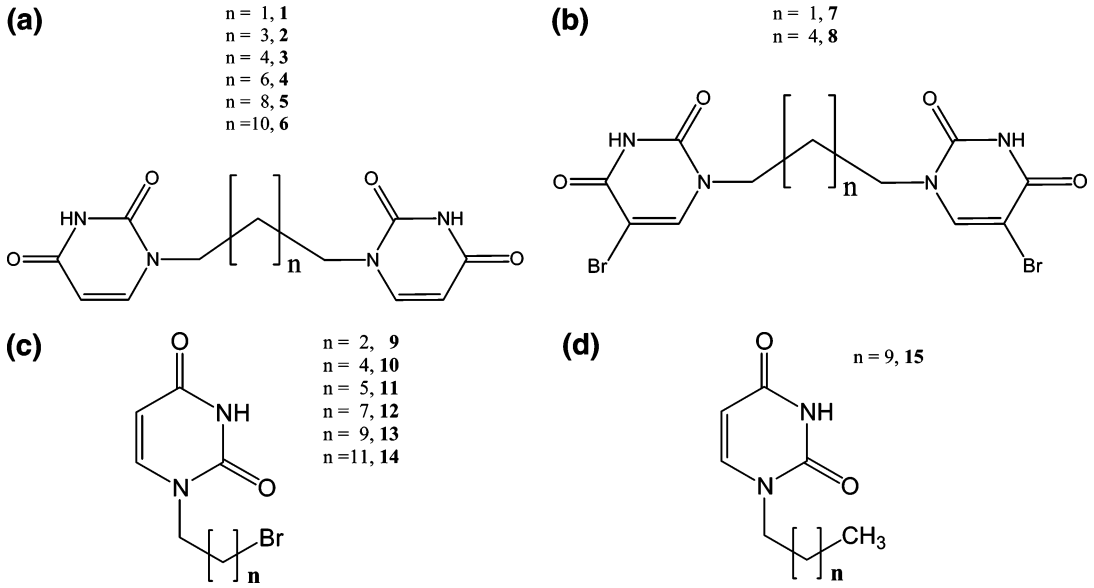

Figure 3. a: Various 1,1′-(α,ω-alkanediyl)bis[uracil] species synthesized and tested. b: Two 1,1′-(α,ω-alkanediyl)bis[5-bromouracil] species synthesized and tested. c: Various 1-(ω-bromoalkyl)uracil species synthesized and tested. d: 1-Undecyl uracil synthesized and tested.

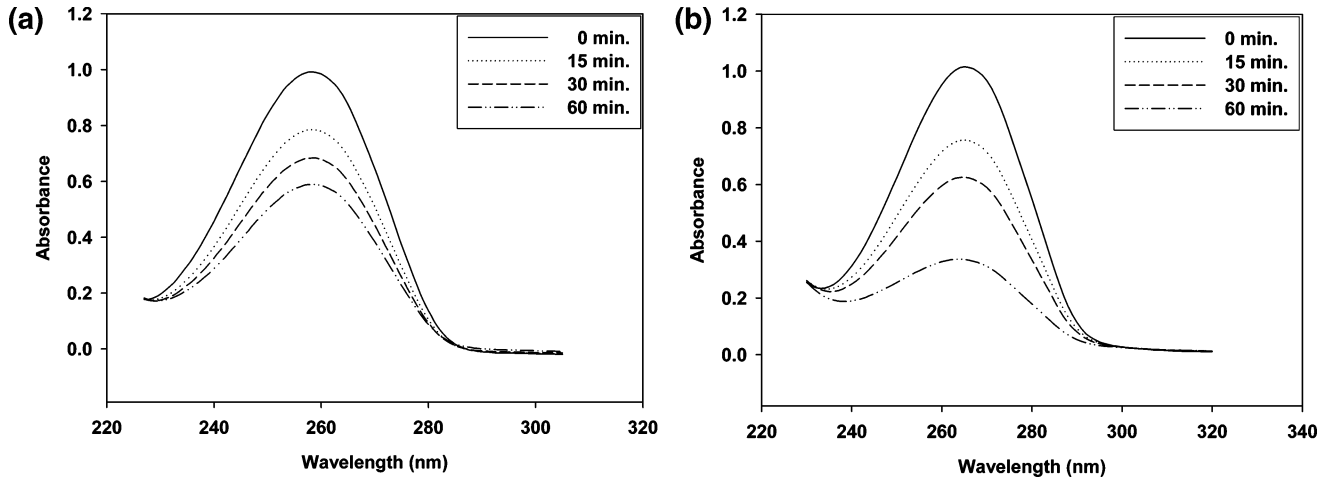

Figure 4. a: Absorption of uracil in water, before irradiation and after 15, 30, and 60 min of irradiation. b: Absorption of 1,1′-(1,3-propanediyl)bis[uracil] in water, before irradiation and after 15, 30, and 60 min of irradiation.

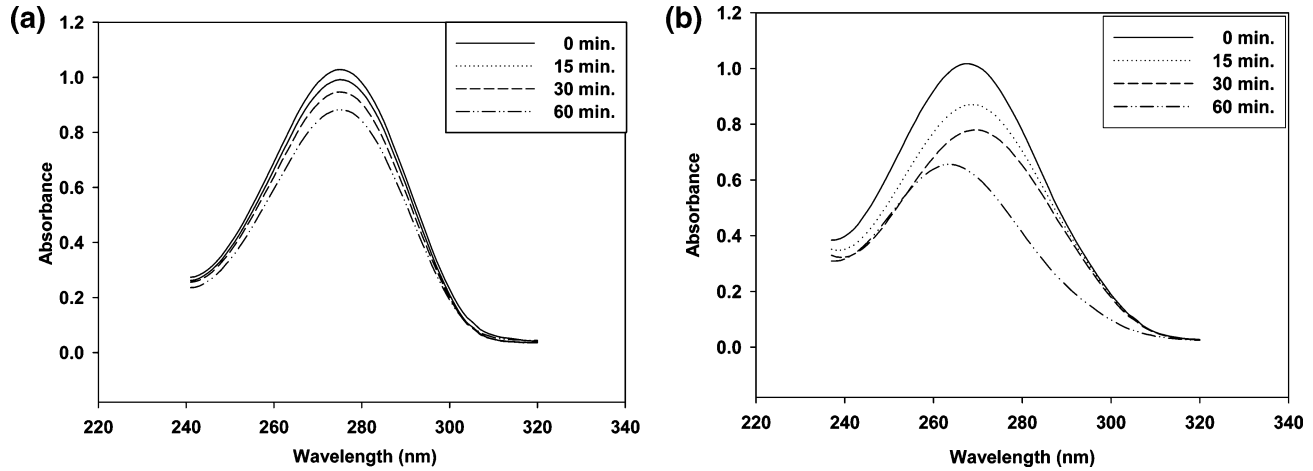

Figure 5. a: Absorption of 5-bromouracil in water, before irradiation and after 15, 30, and 60 min of irradiation, showing no dehalogenation. b: Absorption of 1,1′-(1,3-propanediyl)bis[5-bromouracil] in water, before irradiation and after 15, 30, and 60 min of irradiation, showing significant dehalogenation.

tides.[2] The dimerization efficiency of 5-bromouracil is shown in Figure 5a, and here no dehalogenation was observed. **7** and **8** were prepared and tested, and an improvement in dimerization efficiency was observed, compared to 5-bromouracil in Figure 5a. Unfortunately both **7** and **8** showed significant dehalogenation, as can be seen here for **7** in Figure 5b.

The absorption values (λ_{max}) of the compounds **1**−**6** and **9**−**14** are collected in Figure 6a for the 1,1′-(α,ω-alkanediyl)-

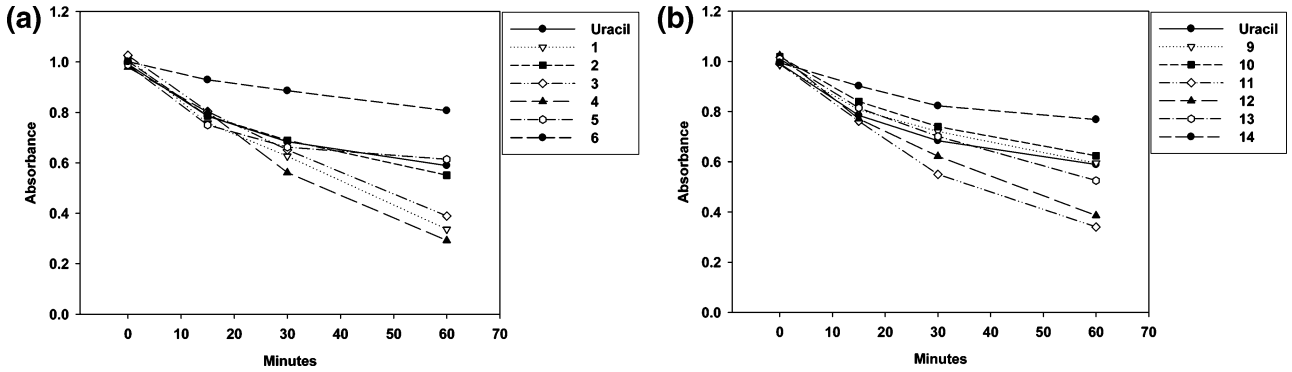

Figure 6. 1,1′-(α,ω-Alkanediyl)bis[pyrimidine] (a) and 1-(ω-bromoalkyl)pyrimidine (b) species before irradiation and after 15, 30, and 60 min of irradiation.

bis[uracil] species and the 1-(ω-bromoalkyl)uracil species in Figure 6b, respectively, and display the absorbance values plotted against time at 0, 15, 30, and 60 min. The 1,1′-(α,ω-alkanediyl)bis[5-bromouracil] and 1-undecyl uracil are left out, **7** and **8** due to dehalogenation and **15** due to deviation in the terminal, having $-CH_3$ instead of $-Br$. Also it was not possible to perform dimerization efficiency experiments on **15** because of crystallization and poor film quality. The compounds showing good dimerization efficiency, the 1-(ω-bromoalkyl)uracil species (**11** and **12**) and the 1,1′-(α,ω-alkanediyl)bis[uracil] species (**1**, **3**, and **4**), were then synthesized in larger portions, for film casting, and tested with UV laser to study their application for optical data storage.

Theory for the Dynamics of Photodimerization Processes in Films. A theory for the dynamics of photodimerization processes in films of arbitrary thickness has been developed by Tomlinson and co-workers.[14] In their model, a film of thickness d is irradiated with a uniform light beam of flux F_0 photons/(cm^2•s) at time $t = 0$. The molecules are characterized by two stable states, labeled a and b with a representing the monomers before irradiation and b representing the final state in which the photoinduced dimers are in equilibrium with monomers. The interaction cross section of molecules in state a is defined to be $s_a(\lambda)$ and is given by the product of the absorption cross section and the quantum efficiency for placing the molecule in state a. Corresponding quantities are defined for the state b. The film with thickness d is irradiated at time $t = 0$ with a uniform light beam of flux F_0. A normalized exposure ρ given by

$$\rho(z,t) = (s_a + s_b)\int_0^t F(z,t')\,dt' \qquad (1)$$

and a normalized exposure at the front face of sample T given by

$$T = (s_a + s_b)F_0 t \qquad (2)$$

are also defined where F is the flux of photons at time t, at a depth of the film z.

Defining $\alpha = \alpha_s/\alpha_i$ as the ratio of absorption of the sample in the initial state and the absorption in the final state, the transmission through the sample is given as

$$\mathrm{Tr} = \left.\frac{(1-\alpha)(1-\exp(-\rho)) + \alpha\rho}{(1-\alpha)(1-\exp(-T)) + \alpha T}\right|_{z=d} \qquad (3)$$

It is assumed here that the matrix itself has no absorption in the region of interest. Experimentally, the only value that needs to be determined is α. The normalized exposure, ρ, is obtained by numerically solving the differential equation

$$\frac{d\rho(z,t)}{dz} = -(\alpha_i(z) - \alpha_s)(1 - \exp[-\rho(z,t)]) - \alpha_s\rho(z,t) \qquad (4)$$

Because the value of α and the flux of photons F_0 are known, the quantity T is just a function of real time. By matching the experimentally obtained transmission as a function of time with the simulated transmission, a value for the absorption cross section may be obtained.

Film Measurements. The absorption spectrum of a 2.4 μm thick film of 1,1′-(1,8-octanediyl)bis[uracil] before and after irradiation at 257 nm is shown in Figure 7. An isosbestic point is obtained at 290 nm. As discussed later, these measurements have been used to estimate the change in refractive index through Kramers−Kronig relations.

Experimentally measured transmission for films of 1,1′-(1,8-octanediyl)bis[uracil] is shown as a function of time in Figure 8. The $1/e^2$ width of the beam was 2 mm. The transmission increases from an initial 1% to over 70% in approximately 20 s. As shown by Kinoshita et al.[15] the quantum efficiency for the process can be calculated with the following equation:

$$\ln\left(\frac{T}{1-T}\right) - \ln\left(\frac{T_0}{1-T_0}\right) = 2.3 \times 10^3 I_0 \epsilon \Phi t \qquad (5)$$

In this equation, T is the transmission of the film at time t, T_0 is the initial transmittance of the film, ϵ is the molar extinction coefficient determined from the absorption spectrum of a known concentration of the material, and Φ is the quantum efficiency. I_0 is the photon flux expressed in einstein cm^{-2} s^{-1}. The molar extinction coefficient was determined to be 5.35×10^3 L mol^{-1} cm^{-1} at a wavelength of 257 nm. From the initial slope of the transmission curve, the quantum yield for dimerization was determined to be 0.21.

With an experimentally determined value for $\alpha = 0.132$ and a flux of 9×10^{16} photons cm^{-2} s^{-1}, the best match to

(14) (a) Tomlinson, W. J.; Chandross, E. A.; Fork, L.; Pryde, C. A.; Lamola, A. A. *Appl. Opt.* **1972**, *11*, 533−548 (b) Tomlinson, W. J. *Appl. Opt.* **1972**, *11*, 823−831. (c) Tomlinson, W. J. *Appl. Opt.* **1976**, *15*, 821−826.

(15) Kinoshita, K.; Horie, K.; Morino, S.; Nishikubo, T. *Appl. Phys. Lett.* **1997**, *70*, 2940−2942.

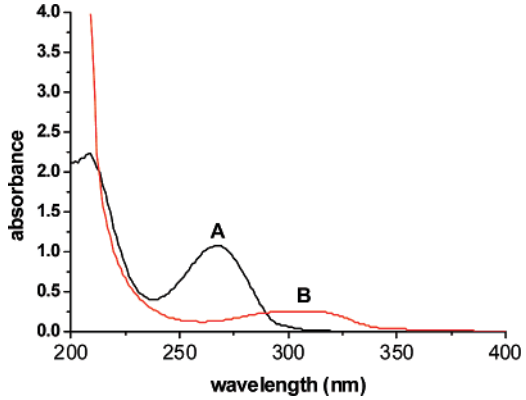

Figure 7. Absorption spectrum of 1,1′-(1,8-octanediyl)bis[uracil] (A) before and (B) after irradiation at 257 nm.

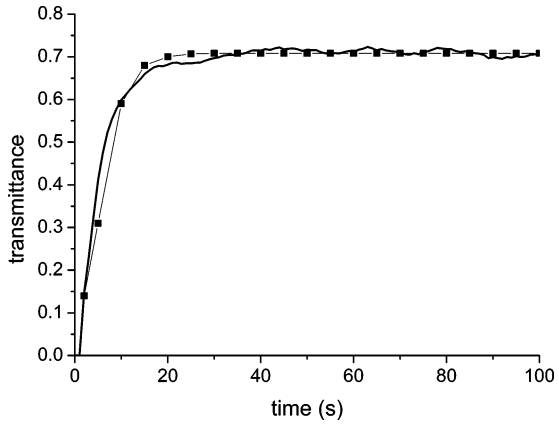

Figure 8. Transmission through a thin film of 1,1′-(1,8-octanediyl)bis-[uracil] as a function of time. The solid curve is the experimental measurement, while the line joining the squares is the simulated curve.

the initial slope of the experimental data is obtained when $s_a + s_b = 4 \times 10^{-18}$ cm^2.

The simulated transmission curve is shown as the line connecting squares in Figure 8. The absorption cross section is estimated to be 0.85×10^{-18} cm^2. There is a slight mismatch between the theory and experiment as a result of a distribution in the quantum efficiency for dimerization. The alignment of the monomers in the matrix will vary from location to location, resulting in a range of quantum efficiencies.

Gray Scale Recording. The large transmission change through the film on irradiation can be used to record multilevel bits, increasing the storage capacity significantly. An example of a 3-bit recording is shown in Figure 9. A 3-bit recording corresponds to recording eight levels of gray. A weakly focused (0.5 mm) laser beam at 257 nm was used for the recording. The power of the laser beam was 0.5 mW, corresponding to an intensity of 250 mW/cm^2. After the desired transmittance was reached, the film was translated unidirectionally to record the other "bits". After the recording, the intensity was decreased to 3 mW/cm^2 and the "bits" were read-out.

Holographic Grating Recording. Holographic gratings have also been recorded in a thin film of 1,1′-(1,8-octanediyl)bis[uracil]. Figure 10 shows the experimental setup. A frequency doubled argon laser at 257 nm is used as the source.

The 257 nm beam from the laser is divided into two by a polarization beam splitter. Each of the beams passes through

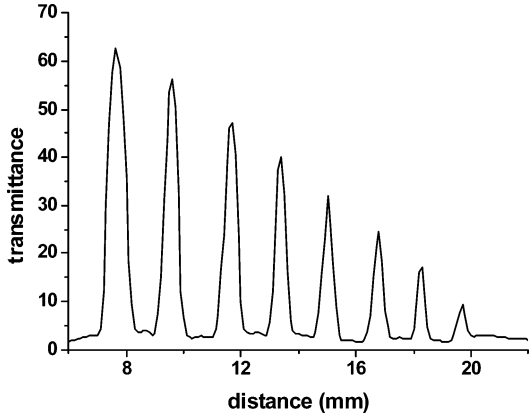

Figure 9. Example of gray scale recording in a film of 1,1′-(1,8-octanediyl)-bis[uracil].

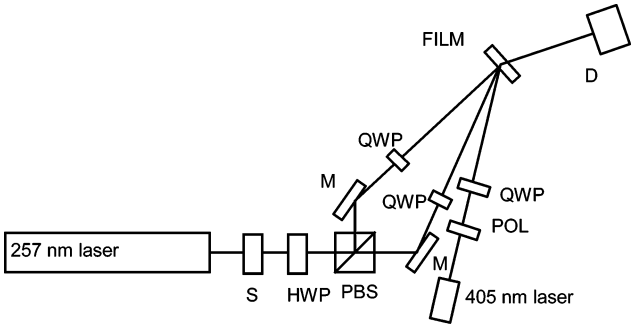

Figure 10. Experimental setup to record diffraction gratings.

a quarter wave plate oriented such that the two beams have the same circular polarization. A half-wave plate in front of the beam splitter can be adjusted to give equal intensities in the two beams for a modulation ratio of 1. The grating is read-out with a 3 mW laser operating at 405 nm. The grating period is 2.5 μm. Figure 11 shows the diffracted power from such a grating read with a 405 nm laser as a function of time. The same graph shows the decrease in transmission of one of the writing beams at 257 nm during the irradiation process. The transmission increases to a maximum of approximately 71% and then starts to decrease; however, the diffraction efficiency continues to increase and reaches 18% at 6000 s. The decrease in the transmission of the 257 nm direct beam is attributed to the formation of a surface relief grating, which strongly diffracts the UV beam away from the detector.

To confirm the presence of the surface relief, the irradiated area was scanned with an atomic force microscope. Figure 12 shows the result of such a scan. The scanned area is 20 $\times$ 20 μm. The maximum surface relief obtained is 200 nm. The surface relief arises because of the change in the dimensions of the film on dimerization.

From the observed absorption spectra shown in Figure 7, we estimated the change in the refractive index as a function of wavelength through Kramers−Kronig relations.[16] A maximum refractive index change of 0.02 was obtained at 290 nm. The calculated diffraction efficiency at 400 nm for the case of a thin absorptive grating[17] was approximately

(16) Ohta, K.; Ishida, H. *Appl. Spectrosc.* **1988**, *42*, 952−957.
(17) Collier, R. J.; Bruckhardt, C. B.; Lin, L. H. *Optical Holography*; Academic Press: London, 1971.

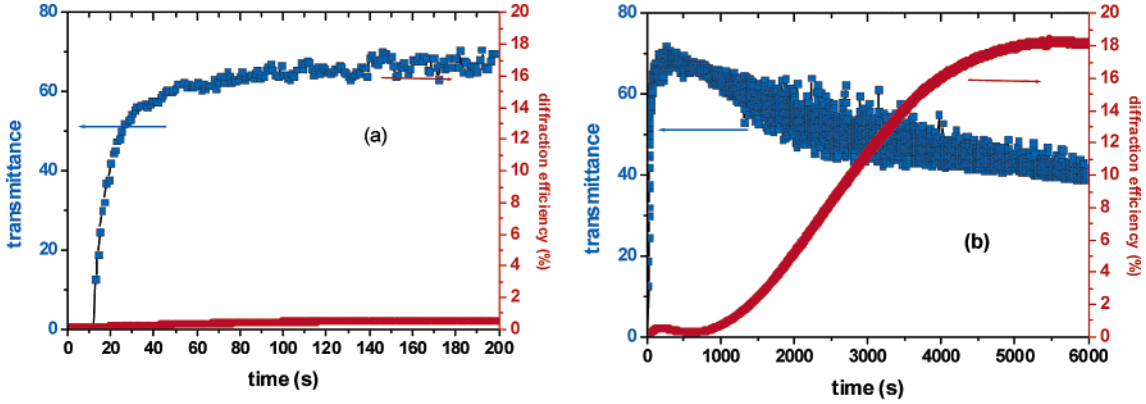

Figure 11. Diffraction efficiency and transmission through a thin film of 1,1′-(1,8-octanediyl)bis[uracil] (a) for short irradiation time and (b) for a long irradiation time.

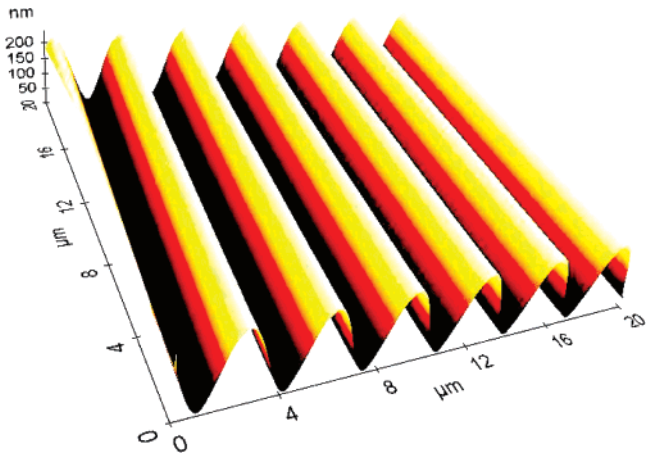

Figure 12. Atomic force microscope scan of the diffraction grating in a film of 1,1′-(1,8-octanediyl)bis[uracil].

0.03%. Thus the contribution of the absorptive gratings at this wavelength is appreciably smaller than the diffraction efficiency due to the surface relief grating. Figure 13 shows the change in the refractive index (left *y* axis) and the diffraction efficiency (right *y* axis) obtained with the Kramers−Kronig relations.

Discussion

Photodimerization reactions in pyrimidines, whether it is in films, crystals, or solutions, have been investigated extensively by Inaki and co-workers[18] over the last two decades. The extensive work of Inaki et al. has been done primarily with thymine, as the chromophore of choice, but our work with uracil has so far been quite consistent with Inaki et al. and their work. Although we have not isolated and characterized the photodimerization products using X-ray crystallography, we are confident that the dimerization takes place through the C-5, C-6 bond of uracil as shown for our system in Figures 1 and 2 and involves the formation of a cyclobutane ring as it has been proven for thymine.[18,19] The electronic properties of the C-5 and C-6 atoms/groups and their significance regarding photodimerization efficiency was investigated previously.[2a] Another significant hindrance for good photodimerization efficiency arises in dilute solutions such as ours due to the fact that the excited-state lifetime of the bases is most often small, compared to the diffusion processes in the solution.[20] Uracil has a larger photodimerization efficiency relative to thymine, primarily because singlet uracil undergoes intersystem crossing more efficiently than singlet thymine, and furthermore a smaller fraction of the metastable uracil adducts fall apart.[21] We have shown that by bringing the chromophores closer to each other, the probability for cycloaddition is increased, and this minimizes the diffusion effect. The reason for the poor dimerization efficiency of some compounds could be explained by the fact that most of the chromophores that absorb a photon revert from the excited state back into the ground state due to a lifetime of only $\sim 10^{-12}$ s, but a small amount manage to reach a long-lived triplet state.[22]

It is also evident from the results that the factor of chain length plays an important role, when viewing the dimerization efficiency and its dependency on the number of methylene groups. The correlation between the number of methylene groups in the 1-(ω-bromoalkyl)uracil species and the 1,1′-(α,ω-alkanediyl)bis[pyrimidine] species and the dimerization efficiency is shown in Figure 14. For the 1-(ω-bromoalkyl)uracil species the case was quite clear: **1** and **2** both had poor dimerization efficiency, but **3** containing six methylene chains was the best, steadily decreasing until reaching **6** as the poorest. For the 1,1′-(α,ω-alkanediyl)bis-[pyrimidine] species it was different, starting with **9** having a good dimerization efficiency, then declining to **10** and increasing again to the top with **12** and declining again until reaching **14**, as the poorest. Except for **9**, there is a clear tendency of six to eight methylene groups being the optimal chain length. No further investigation was done on the 5-bromouracil species due to the dehalogenation process. As for the 1-undecyl uracil due to poor solubility in water,

(18) (a) Kita, Y.; Inaki, Y.; Takemoto, K. *J. Polym. Sci.* **1980**, *18*, 427−439. (b) Suda, Y.; Inaki, Y.; Takemoto, K. *J. Polym. Sci.* **1983**, *21*, 2813−2832. (c) Inaki, Y.; Moghaddam, M. J.; Kanbara, K.; Takemoto, K. *J. Photopolym. Sci. Technol.* **1988**, *1*, 28−35. (d) Moghaddam, M. J.; Hozumi, S.; Inaki, Y.; Takemoto, K. *Polym. J.* **1989**, *21*, 203−213. (e) Moghaddam, M. J.; Kanbara, K.; Hozumi, S.; Inaki, Y.; Takemoto, K. *Polym. J.* **1990**, *22*, 369−380. (f) Inaki, Y. *CRC Handbook of Organic Photochemistry and Photobiology*; 2nd ed.; CRC Press: Boca Raton, FL, 2004; Chapter 104, pp 104-1−104-34.

(19) Pullman B. *Photochem. Photobiol.* **1968**, *7*, 525−530.
(20) Pechenaya, V. I.; Danilov, V. I.; Slyusarchuk, O. N.; Alderfer, J. L. *Photochem. Photobiol.* **1995**, *61* (5), 435−441.
(21) Wagner, P. J.; Bucheck, D. J. *J. Am. Chem. Soc.* **1970**, *92* (1), 181−185.
(22) Hauswirth, W.; Daniels, M. *Chem. Phys. Lett.* **1971**, *10*, 140−144.

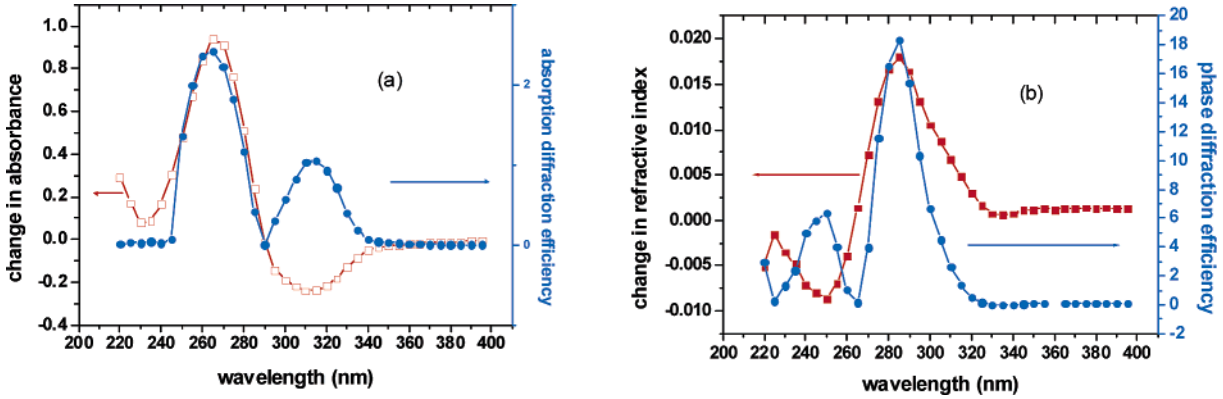

Figure 13. Calculated refractive index change due to a change in the transmission based on Kramers−Kronig relations and the calculated diffraction efficiency: (a) absorptive diffraction grating and (b) phase diffraction grating.

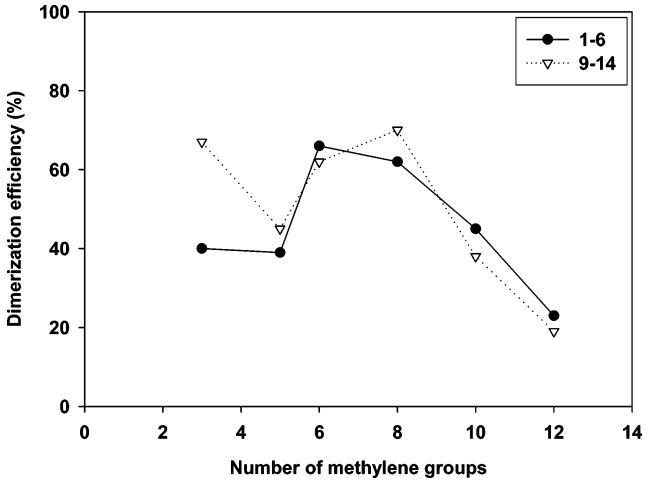

Figure 14. Dimerization efficiency and its dependency on the number of methylene groups for **1**−**6** and **9**−**14** in solution.

crystallization in solution and in film was observed. This has also been observed in the literature for thymine, and this is also the case for thymine species with fewer methylene groups.[18]

Conclusion

We have presented a new possible optical data storage medium, based on photodimerization using UV laser technology. **4** is the best suited of the synthesized compounds, due to the fact that it had the best dimerization efficiency. The film quality of **4** is excellent, and the film is resistant (without any protective layers) to cold (−25 °C), heat (150 °C), moisture, and sunlight. The film is easy to cast and becomes hard and not easily scratched after it has been dried in the oven for 1 h at 100 °C, making it suitable for coating on disks.

When our starting point is taken as 25 gigabytes on a 5.25 in. disk with a 405 nm laser source and a 0.85 numerical aperture (NA) optics as specified for the recent Blu-Ray system (with all the redundant storage for recoding, error correction, etc.), a 2.5 times increase in the storage capacity can be achieved through the use of the 250 nm laser as the light source, with the same NA. We have shown that a further increase by a factor of 3 is possible using a gray-level storage. Thus theoretically it should be possible to increase the storage capacity to more than 150 GB on a CD.

The smallest achievable spot size is given by $s = \lambda/\mathrm{NA}$, where λ is the wavelength of light. For a 250 nm source and 0.85 NA aperture optics, this is approximately 300 nm. Assuming that the photon flux is the same (9×10^{16} photons $\mathrm{cm}^{-2}\ \mathrm{s}^{-1}$) and the response of the material is linear, the time required for approximately 10% transmission change (corresponding to a 3-bit storage) is estimated to be 45 ns, and for an 80% change it is estimated to be 450 ns. The energy densities in these cases turn out to be 0.3 $\mathrm{J/cm}^2$ to 3 $\mathrm{J/cm}^2$. We are not able to verify experimentally whether the material has a damage threshold greater than this; however, from the literature, typical laser fluences of "tens of $\mathrm{mJ/cm}^2$ to more than 1 $\mathrm{J/cm}^2$" are required for laser damage at 250 nm.[23] Thus, to improve the writing speed as well as the damage threshold, it is imperative to find materials with even larger photodimerization cross-sections.

Experimental Section

Melting point measurements were done on a Büchi SMP-20 apparatus. NMR spectra were recorded on a Bruker 250 MHz/52MM apparatus. Irradiation of the compounds in solution was done using a UV lamp, Spectroline model ENF-260C/FE (CM-10), and spectra were recorded on a Shimadzu UV-1700 spectrophotometer. The irradiation of the films was done using a frequency doubled argon laser at 257 nm. Matrix-assisted laser desorption ionization time-of-flight (MALDI-TOF) mass spectra were recorded on a Bruker Reflex IV, using the following method: Reflectron MALDI-TOF with pulsed ion extraction and positive ion analysis were used, where the sample was either applied pure or mixed with potassiumtrifluoracetate (31 mg/5 mL MeOH) or 1 M 1,8,9-trihydroxyanthracene (dithranol) as the matrix reagent. TLC was done in the solvent system ethyl acetate/methanol (20:1, v/v, ratio), using ALUGRAM SIL G/UV_{254} 0.20 mm silica gel 60. The column chromatography was done using a gradient solvent system ethyl acetate/methanol (40:1, v/v ratio), slowly increasing and ending at a 100% methanol. For this purpose we used silica gel 60 (0.015−0.040 mm) from MERCK. GCMS was done on a HP 6890 series mass selective detector, GC system, and injector.

Mass Spectrometry. Fragmentation patterns involving the uracil nuclei agreed well with those reported in the literature.[24] Fragmentation of the polymethylene chain was favored over cleavage of the uracil nucleus. Intense peaks could be assigned in good agreement with the fragments expected to be observed: *m/e* 112, (uracil), *m/e* 42 ($-CH_2-CH_2-CH_2^+$), *m/e* 80/82 (HBr^+), *m/e* 79/

(23) Lippert, J.; Dickinson, J. T. *Chem. Rev.* **2003**, *103*, 453−485.
(24) Rice, J. M.; Dudek, G. O.; Barber, M. *J. Am. Chem. Soc.* **1965**, *87*, 4569−4576.

81 (Br^+), *m*/*e* 107/109 ($CH_2-CH_2-Br^+$), and *m*/*e* 121/123 ($-CH_2-CH_2-CH_2-Br^+$). Products formed by chemical intramolecular cyclization were observed in the spectra (*m*/*e* 152), and these products have been discussed in the literature.[5]

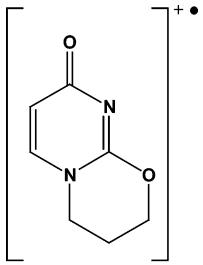

m/e 152

The same fragmentation pattern was found in the majority of the spectra, indicating that the breaking of the bonds was favorable in the same areas despite the length of the methylene chains: *m*/*e* 152 (uracil-$C_3H_5^+$), *m*/*e* 139 (uracil-$C_2H_4^+$), *m*/*e* 126 (uracil-CH_3^+), *m*/*e* 112 (uracil-H^+), *m*/*e* 109 (uracil-$C_3H_5^+$ − HNCO, *m*/*e* 69 uracil-H^+ − HNCO), and *m*/*e* 55 (uracil-CH_3^+ − HNCO and − CO).

Preparation of 1,1′-(α,*ω*-Alkanediyl)bis[pyrimidine] Species, Using *t*-BuOK. Into a solution of uracil or 5-bromouracil (10 mmol) in DMF (150 mL) were added *t*-BuOK (10 mmol) and $Br(CH_2)_n$-Br (n = 3−12; 10 mmol). The mixture was stirred at room temperature for 2−3 days. The resulting mixture was evaporated to give a residue, which was submitted to chromatography over silica gel. By elution of a mixture of ethyl acetate and hexane, 1-(*ω*-bromoalkyl)uracil or 1-(*ω*-bromoalkyl)-5-bromouracil was obtained. Further elution with a mixture of ethyl acetate and methanol gave 1,1′-(α,*ω*-alkanediyl)bis[uracil] or 1,1′-(α,*ω*-alkanediyl)bis[5-bromouracil].[9]

Preparation of 1-(*ω*-Bromoalkyl)pyrimidine Species, Using TMP. Into a solution of uracil or 5-bromouracil (10 mmol) in dry DMF (150 mL) were added TMP (10 mmol), and $Br(CH_2)_nBr$ (n = 3−12; 10 mmol). The mixture was stirred at room temperature for 24 h. The resulting mixture was evaporated to give a residue, which was submitted to chromatography over silica gel. By elution of a mixture of ethyl acetate and methanol, 1-(*ω*-bromoalkyl)uracil or 1-(*ω*-bromoalkyl)-5-bromouracil were isolated in good purity.

Preparation of 1-Undecyl Uracil, Using K_2CO_3. 1-Undecyl uracil **15** was prepared by dissolving 18 mmol uracil in 10 mL of DMF, and K_2CO_3 was added. Then 18 mmol 1-bromo-undecane was dissolved in 10 mL of DMF by adding dropwise at 45 °C under stirring for 24 h. The reaction was followed by TLC (1:1 ethyl acetate/*n*-heptane). A liquid column chromatography was done using kiselgel 60 and the same solvent system as for TLC. Pure 1-undecyl uracil was obtained after evaporation, and re-crystallization gave transparent square plated crystals (yield 68%).

Preparation of Films. A quartz plate was cleaned thoroughly, and approximately 1 mg of compound was dissolved in a 1% solution of (3-(methylamino)propyl)-trimethoxysilane, in Milli-Q water. Then the mixture was filtered through a 0.22 μm filter, Millex-GS, applied directly onto the cleaned quartz plate, and finally inserted into an oven for 1 h at 100 °C, giving excellent films.

1,1′-(α,*ω*-Alkanediyl)bis[uracil]. ***1****, 1,1′-(1,3-Propanediyl)bis-[uracil].* ^{1}H NMR (DMSO-d_6) δ: = 11.20 (broad, 2H, NH), 7.65 (d, 2H, J = 8 Hz), 5.53 (dd, 2H, J = 8 Hz, J = 2 Hz), 3.67 (t, 4H, J = 7.2 Hz), 1.92 (quintet, 2H, J = 7.2 Hz). ^{13}C NMR (DMSO-d_6) δ: 163.66, 150.86, 145.57, 100.77, 46.93, 25.26. MALDI-TOF MS (*m*/*z*): $(C_{11}H_{12}N_4O_4 + K)^+$ calcd, 303.34; found, 303.09. Mp 284−286 °C (lit.[5] 289−293 °C and lit.[9] 280−285 °C).

2*, 1,1′-(1,5-Pentanediyl)bis[uracil].* ^{1}H NMR (DMSO-d_6) δ: 11.22 (broad, 2H, NH), 7.63 (d, 2H, J = 8 Hz), 5.53 (dd, 2H, J = 8 Hz, J = 2 Hz), 3.62 (t, 4H, J = 7.2 Hz), 1.57 (broad quintet, 4H, J = 7.2 Hz), 1.22 (broad quintet, 2H, J = 7.2 Hz). ^{13}C NMR (DMSO-d_6) δ: 163.63, 150.86, 145.57, 100.77, 46.93, 27.26, 22.51. MALDI-TOF MS (*m*/*z*): $(C_{13}H_{16}N_4O_4 + K)^+$ calcd, 331.39; found, 331.41. Mp 247−249 °C (lit.[9] 246−248 °C).

3*, 1,1′-(1,6-Hexanediyl)bis[uracil].* ^{1}H NMR (DMSO-d_6) δ: 11.22 (broad, 2H, NH), 7.67 (d, 2H, J = 8 Hz), 5.55 (dd, 2H, J = 8 Hz, J = 2 Hz), 3.69 (t, 4H, J = 7.2 Hz), 1.60−1.50 (broad, 4H), 1.30−1.20 (broad 4H). ^{13}C NMR (DMSO-d_6) δ: 163.63, 150.86, 145.57, 100.77, 46.93, 28.26, 25.51. MALDI-TOF MS (*m*/*z*): $(C_{14}H_{18}N_4O_4 + H)^+$ calcd, 307.33; found, 307.19. Mp 244−246 °C (lit.[9] 242−245 °C).

4*, 1,1′-(1,8-Octanediyl)bis[uracil].* ^{1}H NMR ($CDCl_3$) δ: 8.82 (broad, 2H, NH), 7.15 (d, 2H, J = 8 Hz), 5.75 (dd, 2H, J = 8 Hz, J = 2 Hz), 3.72 (t, 4H, J = 7.2 Hz), 1.59 (broad quintet, 4H, J = 7.2 Hz), 1.4−1.25 (m, 8H). ^{13}C NMR ($CDCl_3$) δ: 163.63, 150.86, 144.57, 102.77, 48.93, 29.26, 28.51, 26.31. MALDI-TOF MS (*m*/*z*): $(C_{16}H_{22}N_4O_4 + H)^+$ calcd, 335.38; found, 335.33. Mp 190−193 °C.

5*, 1,1′-(1,10-Decanediyl)bis[uracil].* ^{1}H NMR ($CDCl_3$) δ: 8.30 (broad, 2H, NH), 7.15 (d, 2H, J = 8 Hz), 5.69 (dd, 2H, J = 8 Hz, J = 2 Hz), 3.70 (t, 4H, J = 7.2 Hz), 1.66 (quintet, 4H, J = 7.2 Hz), 1.4−1.23 (m, 12H). ^{13}C NMR ($CDCl_3$) δ: 163.43, 150.76, 144.37, 102.07, 48.83, 29.16, 28.91, 29.01, 26.24. MALDI-TOF MS (*m*/*z*): $(C_{18}H_{26}N_4O_4 + K)^+$ calcd, 401.52; found, 401.51. Mp 158−161 °C (lit.[9] 158−159 °C).

6*, 1,1′-(1,12-Dodecanediyl)bis[uracil].* ^{1}H NMR ($CDCl_3$) δ: 8.29 (broad, 2H, NH), 7.13 (d, 2H, J = 8 Hz), 5.68 (dd, 2H, J = 8 Hz, J = 2 Hz), 3.71 (t, 4H, J = 7.2 Hz), 1.66 (quintet, 4H, J = 7.2 Hz), 1.4−1.25 (m 16H). ^{13}C NMR ($CDCl_3$) δ: 163.75, 150.86, 144.57, 102.27, 49.03, 29.26, 29.01, 29.23, 26.35. MALDI-TOF MS (*m*/*z*): $(C_{20}H_{30}N_4O_4 + H)^+$ calcd, 391.49; found, 391.53. Mp 136−141 °C.

1,1′-(α,*ω*-Alkanediyl)bis[5-bromouracil]. ***7****, 1,1′-(1,3-Propanediyl)bis[5-bromouracil].* ^{1}H NMR (DMSO-d_6) δ: 13.02 (broad s, 2H, NH), 8.37 (s, 2H), 3.65 (t, 4H, J = 7.2 Hz), 1.90 (quintet, 2H, J = 7.2 Hz). ^{13}C NMR (DMSO-d_6) δ: 160.16, 150.86, 145.87, 95.07, 44.75, 27.86. MALDI-TOF MS (*m*/*z*): $(C_{11}H_{10}Br_2N_4O_4 + K)^+$ calcd, 461.13; found, 461.20. Yellow oil.

8*, 1,1′-(1,6-Hexanediyl)bis[5-bromouracil].* ^{1}H NMR (DMSO-d_6) δ: 13.05 (broad s, 2H, NH), 8.32 (s, 2H), 3.67 (t, 4H, J = 7.2 Hz), 1.60−1.50 (broad, 4H), 1.30−1.20 (broad 4H). ^{13}C NMR (DMSO-d_6) δ: 160.13, 150.83, 145.85, 95.02, 46.93, 28.26, 25.31. MALDI-TOF MS (*m*/*z*): $(C_{14}H_{16}Br_2N_4O_4 + K)^+$ calcd, 503.21; found, 503.32. Yellow oil.

1-(*ω*-Bromoalkyl)uracil. ***9****, 1-(3-Bromopropyl)uracil.* ^{1}H NMR ($CDCl_3$) δ: 9.30 (broad, 1H, NH), 7.27 (d, 1H, J = 8 Hz), 5.75 (dd, 1H, J = 8 Hz, J = 2 Hz), 3.92 (t, 2H, J = 6.4 Hz), 3.42 (t, 2H, J = 6.4 Hz), 2.29 (quintet, 2H, J = 6.4 Hz). ^{13}C NMR ($CDCl_3$) δ: 163.59, 150.86, 144.57, 102.77, 47.63, 31.04, 29.66. MALDI-TOF MS (*m*/*z*): $(C_7H_9BrN_2O_2 + H)^+$ calcd, 234.07; found, 234.07. Mp 87−89 °C (lit.[5] 87−96 and lit.[9] 88−89 °C).

10*, 1-(5-Bromopentyl)uracil.* ^{1}H NMR ($CDCl_3$) δ: 9.50 (broad, 1H, NH), 7.17 (d, 1H, J = 8 Hz), 5.75 (dd, 1H, J = 8 Hz, J = 2 Hz), 3.72 (t, 2H, J = 7 Hz), 3.42 (t, 2H, J = 7 Hz), 1.92 (quintet, 2H, J = 7 Hz), 1.72 (quintet, 2H, J = 7 Hz), 1.52 (quintet, 2H, J = 7 Hz). ^{13}C NMR ($CDCl_3$) δ: 164.46, 150.86, 144.57, 102.02, 48.43, 33.29, 31.84, 27.96, 24.67. MALDI-TOF MS (*m*/*z*): $(C_9H_{13}BrN_2O_2 + K)^+$ calcd, 300.22; found, 300.24. Mp 78−80 °C (lit.[9] 80−81 °C).

11*, 1-(6-Bromohexyl)uracil.* ^{1}H NMR ($CDCl_3$) δ: 10.05 (broad, 1H, NH), 7.16 (d, 1H, J = 8 Hz), 5.75 (dd, 1H, J = 8 Hz, J = 2 Hz), 3.73 (t, 2H, J = 7 Hz), 3.41 (t, 2H, J = 7 Hz), 1.90 (quintet, 2H, J = 7 Hz), 1.72 (quintet, 2H, J = 7 Hz), 1.50 (quintet, 2H, J

= 7 Hz), 1.37 (quintet, 2H, J = 7 Hz). ^{13}C NMR ($CDCl_3$) δ: 164.56, 151.86, 144.47, 102.77, 48.63, 33.60, 32.04, 28.86, 27.66, 24.63. MALDI-TOF MS (m/z): $(C_{10}H_{15}BrN_2O_2 + H)^+$ calcd, 275.14; found, 275.16. Mp 77−79 °C (lit.[9] 76−77 °C).

12, *1-(8-Bromooctyl)uracil*. ^{1}H NMR ($CDCl_3$) δ: 9.05 (broad, 1H, NH), 7.14 (d, 1H, J = 8 Hz), 5.65 (dd, 1H, J = 8 Hz, J = 2 Hz), 3.72 (t, 2H, J = 7 Hz), 3.42 (t, 2H, J = 7 Hz), 1.82 (quintet, 2H, J = 7 Hz), 1.62 (quintet, 2H, J = 7 Hz), 1.42 (quintet, 2H, J = 7 Hz), 1.37−1.21 (m, 6H). ^{13}C NMR ($CDCl_3$) δ: 163.56, 150.86, 144.47, 102.07, 48.73, 33.90, 32.64, 29.18, 28.96, 28.76, 28.64, 27.63, 27.63. MALDI-TOF MS (m/z): $(C_{12}H_{19}BrN_2O_2 + H)^+$ calcd, 304.21; found, 304.21. Mp 82−85 °C.

13, *1-(10-Bromodecyl)uracil*. ^{1}H NMR ($CDCl_3$) δ: 8.85 (broad, 1H, NH), 7.14 (d, 1H, J = 8 Hz), 5.65 (dd, 1H, J = 8 Hz, J = 2 Hz), 3.72 (t, 2H, J = 7 Hz), 3.42 (t, 2H, J = 7 Hz), 1.82 (quintet, 2H, J = 7 Hz), 1.62 (quintet, 2H, J = 7 Hz), 1.42 (quintet, 2H, J = 7 Hz), 1.38−1.26 (m, 10H). ^{13}C NMR ($CDCl_3$) δ: 163.76, 151.03, 144.47, 102.07, 48.73, 34.04, 32.90, 29.34, 29.30, 29.04, 28.96, 28.76, 28.24, 26.43. MALDI-TOF MS (m/z): $(C_{14}H_{23}BrN_2O_2 + K)^+$ calcd, 370.35; found, 370.38. Mp 73−75 °C (lit.[9] 76−77 °C).

14, *1-(12-Bromododecyl)uracil*. ^{1}H NMR ($CDCl_3$) δ: 8.29 (broad, 1H, NH), 7.13 (d, 1H, J = 8 Hz), 5.67 (dd, 1H, J = 8 Hz, J = 2 Hz), 3.71 (t, 2H, J = 7 Hz), 3.41 (t, 2H, J = 7 Hz), 1.83 (quintet, 2H, J = 7 Hz), 1.63 (quintet, 2H, J = 7 Hz), 1.45−1.20 (m, 16H). ^{13}C NMR ($CDCl_3$) δ: 163.76, 151.86, 134.47, 109.07, 49.73, 41.04, 33.90, 33.34, 32.34, 32.04, 28.16, 26.76, 25.64. MALDI-TOF MS (m/z): $(C_{16}H_{27}BrN_2O_2 + H)^+$ calcd, 360.31; found, 360.30. Mp 75−78 °C.

15, *1-Undecyl Uracil*. ^{1}H NMR ($CDCl_3$) δ: 8.99 (broad, 1H, NH), 7.13 (d, 1H, J = 8 Hz), 5.67 (dd, 1H, J = 8 Hz, J = 2 Hz), 3.71 (t, 2H, J = 7 Hz), 1.63 (quintet, 2H, J = 7 Hz), 1.45−1.20 (m, 16H), 0.88 (t, 3H, J = 6 Hz). ^{13}C NMR ($CDCl_3$) δ: 163.76, 151.06, 144.47, 102.07, 48.73, 31.94, 29.90, 29.24, 29.04, 28.98, 28.16, 26.76, 22.64, 14.1. MALDI-TOF MS (m/z): $(C_{15}H_{26}N_2O_2 + K)^+$ calcd, 305.48; found, 305.55. Yield: 68%. Mp 80−81 °C (platelets).

Acknowledgment. The authors wish to thank synthesis engineer Lizette Bruun for her generous assistance with GCMS and for stimulating discussions. The authors also wish to recognize laboratory technician Lotte Nielsen for her help with MALDI-TOF and Dr. Noemi Rozlosnik for her help with atomic force microscopy. The authors thank the Danish Technical Research Council (STVF) for financial support.

CM061092F